DALTON
FULL PAPER

Reactions of ferrocenylboranes with 2,5-bis(pyridyl)pyrazine and quaterpyridine: charge-transfer complexes and redox-active macrocycles

Li Ding,[a] Kuangbiao Ma,[a] Gerd Dürner,[b] Michael Bolte,[b] Fabrizia Fabrizi de Biani,[c] Piero Zanello[c] and Matthias Wagner*[a]

[a] *Institut für Anorganische Chemie, J.W. Goethe-Universität Frankfurt, Marie-Curie-Strasse 11, D-60439 Frankfurt (Main), Germany. E-mail: Matthias.Wagner@chemie.uni-frankfurt.de*
[b] *Institut für Organische Chemie, J.W. Goethe-Universität Frankfurt, Marie-Curie-Strasse 11, D-60439 Frankfurt (Main), Germany*
[c] *Dipartimento di Chimica dell'Università, Via Aldo Moro, I-53100 Siena, Italy*

Received 3rd December 2001, Accepted 31st January 2002
First published as an Advance Article on the web 26th March 2002

Reactions of FcB(Me)Br [**1**; Fc = $(C_5H_5)Fe(C_5H_4)$] and 1,1′-fc[B(Me)Br]$_2$ [**2**; fc = $(C_5H_4)_2Fe$] with 2,5-bis(pyridyl)-pyrazine (bppz) and 2,2′:4′,4″:2″,2‴-quaterpyridine (qpy) are reported. The pyrazine derivative bppz forms stable boronium cations with **1** and **2** to give the complexes [FcB(Me)bppz]Br, **[1C]Br**, and {1,1′-fc[B(Me)bppz]$_2$}Br$_2$, **[2C$_2$]Br$_2$**. The 4,4′-bipyridine derivative qpy can be used to link two ferrocenylborane moieties together, which gives access to the open-chain dinuclear aggregate [FcB(Me)qpyB(Me)Fc]Br$_2$, **[1D1]Br$_2$**, and to the macrocyclic molecule **[2D]$_2$Br$_4$**. The bppz adducts possess an intense green colour, and the qpy complexes are deeply blue coloured, which is indicative of charge-transfer interactions between the electron-rich ferrocene moieties and their electron-poor aromatic substituents. The hexafluorophosphate salts of all compounds undergo a reversible ferrocene oxidation and several consecutive reduction processes, which are centred at the cationic sidechains.

Introduction

The incorporation of organometallic moieties into polymer skeletons and macrocyclic frameworks is currently attracting growing attention. Applications of the resulting macromolecules lie in the fields of magnetic, electronic and liquid crystalline materials.[1–4] Macrocyclic receptors are used for the selective recognition of small molecules, as well as for the generation of chemical sensors.[5,6]

The development of main-chain metal-containing macromolecules still offers a considerable challenge. Even if an efficient oligomerization reaction has been developed, polymer (macrocycle) synthesis may still be accompanied—or even dominated—by the formation of macrocyclic (polymeric) species. Consequently, there is still demand for synthesis strategies providing selective access to *either* polymeric compounds *or* macrocyclic frameworks.

In an attempt to combine the unique electronic properties of ferrocene building blocks with the efficiency of coordination polymer synthesis, our group has put forward a novel approach, which takes advantage from the spontaneous formation and high directionality of boron–nitrogen bonds.[7–9] The first components required are mono- and 1,1′-diborylated ferrocene derivatives, which are readily accessible following the method of Siebert and coworkers.[10,11] The further reaction of these Lewis acidic organometallics with difunctional Lewis bases (*e.g.* pyrazine, 4,4′-bipyridine) conveniently leads to macromolecular aggregates (*e.g.* **A**, Fig. 1).[7–9] One drawback of **A** was found to be its very poor solubility in all common solvents. Any further processing of the material (*e.g.* formation of thin films to investigate its electronic properties) thus presents considerable difficulties.

Closely related to **A** are compounds **B** (**B1–B3**, Fig. 1) composed of one ferrocene backbone and up to four pendent 2,2′-bipyridylboronium substituents.[12,13] Due to their cationic charge and the chelating coordination mode of the base, **B1–B3** possess high solubility in polar solvents (*e.g.* DMSO, acetonitrile) without dissociation of their B–N bonds.

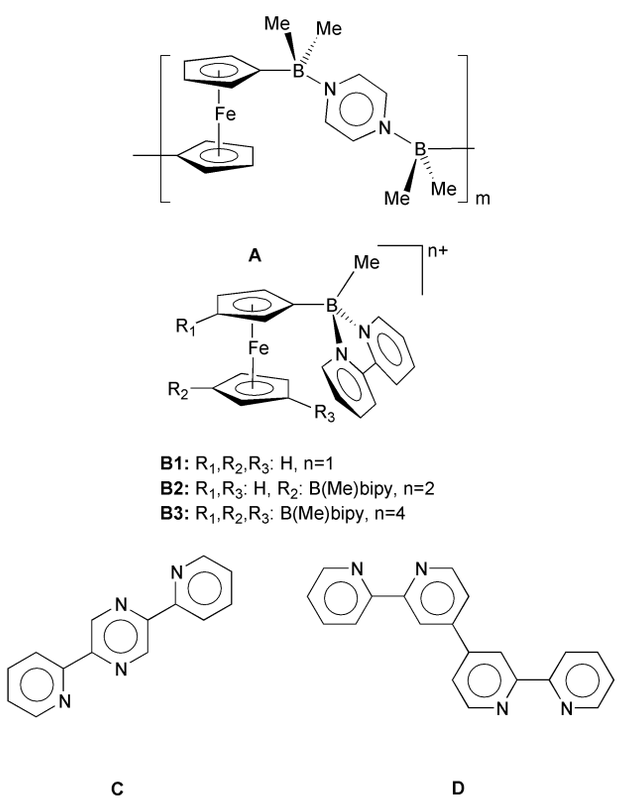

Fig. 1

 DOI: 10.1039/b110993f

Moreover, compounds **B** are able to accept or deliver three (**B1**) to nine (**B3**) electrons, which makes them promising building blocks in the development of novel electron storage media.[12,13]

Our aim is to generate highly redox-active materials combining the polymeric nature of **A** with the high solubility and stability of **B**. In this respect, tetrafunctional Lewis bases 2,5-bis(pyridyl)pyrazine (bppz, **C**)[14] and 2,2′:4′,4″:2″,2‴-quaterpyridine (qpy, **D**)[15] appear to be particularly suitable ligands, since they merge 2,2′-bipyridine subunits with pyrazine and 4,4′-bipyridine functionalities, respectively (Fig. 1).

One focus of this paper lies on the reactions of monoborylated ferrocene **1** with **C** and **D**, which will generate mono- and dinuclear complexes only (Scheme 1).

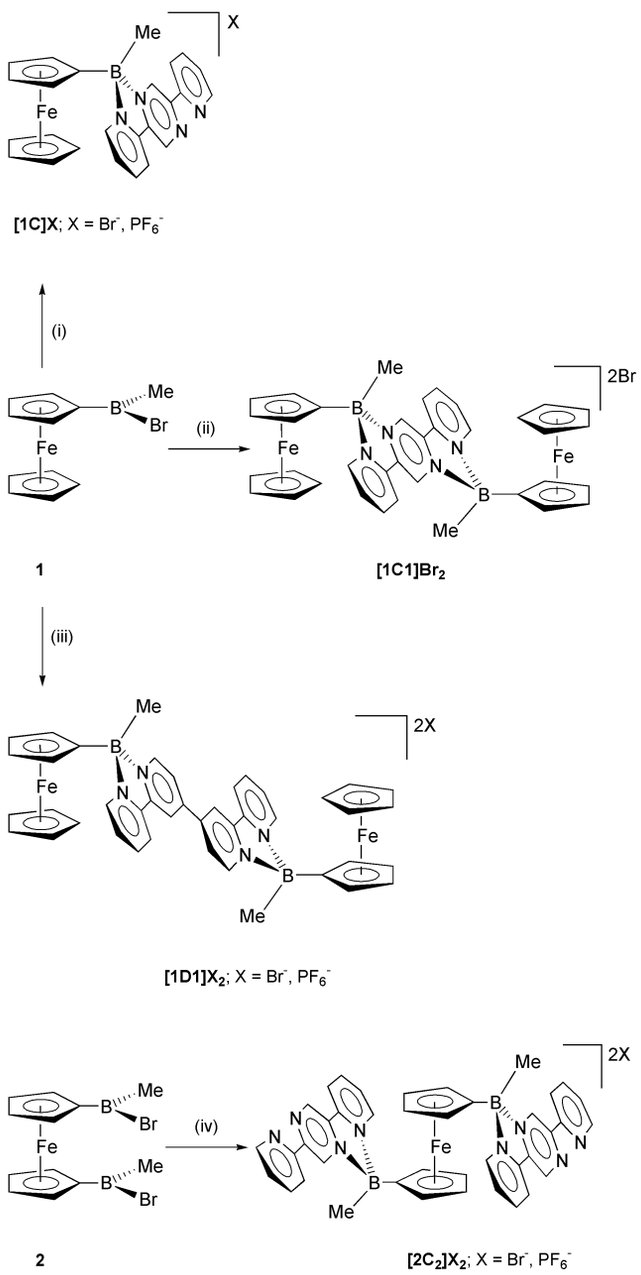

Scheme 1 Synthesis procedures. *Reagents and conditions*: (i) **[1C]PF$_6$**: +1**C** (C_7H_8, room temperature) + excess NH_4PF_6 (H_2O, room temperature). (ii) **[1C1]Br$_2$**: +1/2**C** (CH_2Cl_2, room temperature). (iii) **[1D1](PF$_6$)$_2$**: +1/2**D** (CH_2Cl_2, −78 °C) + excess NH_4PF_6 (H_2O, room temperature). (iv) **[2C$_2$](PF$_6$)$_2$**: +2**C** (C_7H_8, −60 °C) + excess NH_4PF_6 (H_2O, room temperature).

The expected products will supply valuable information about the electrochemical properties and the stability of this class of compounds. Moreover, the reaction of **2** with **C** and **D** will help to evaluate the perspective of our approach regarding the synthesis of ferrocene-containing macromolecules (Scheme 2).

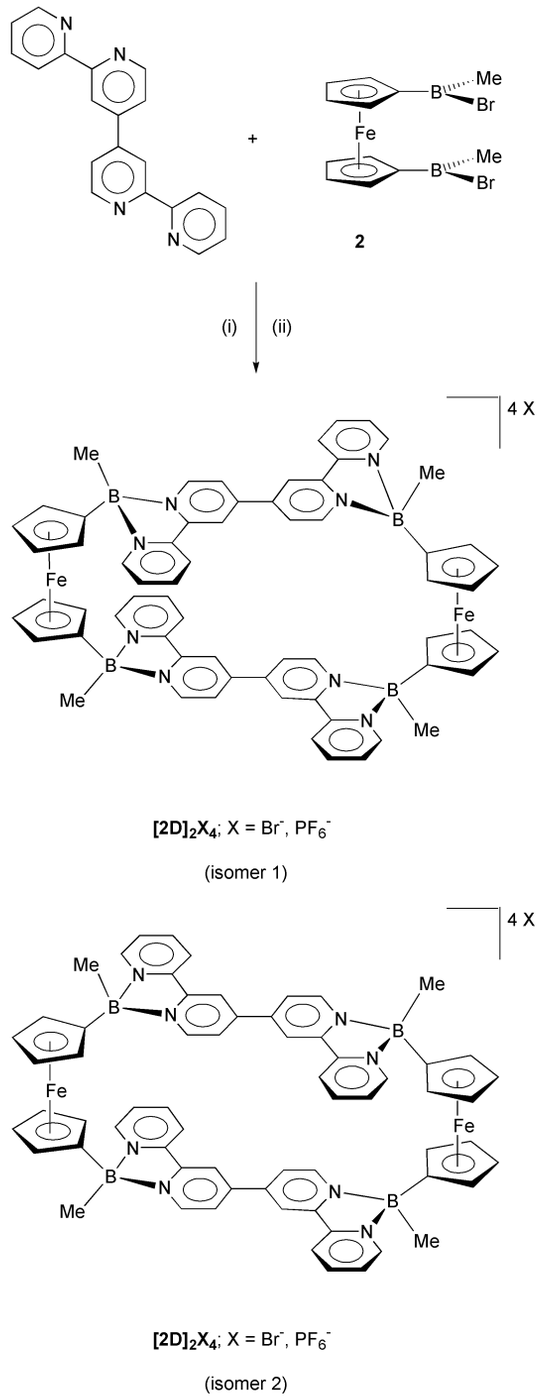

Scheme 2 Synthesis of macrocyclic **[2D]$_2$(PF$_6$)$_4$**. *Reagents and conditions*: (i) CH_2Cl_2, −78 °C; (ii) +4 $TlPF_6$ (CH_3CN, room temperature).

Results and discussion

Syntheses

Reaction of FcB(Me)Br [**1**; Fc: $(C_5H_5)Fe(C_5H_4)$] with one equiv. of ligand **C** in toluene gives green microcrystalline **[1C]Br**. Treatment of **[1C]Br** in water with an excess of NH_4PF_6 leads to the precipitation of the corresponding blue salt **[1C]PF$_6$**. Using a similar procedure, the green adduct **[2C$_2$](PF$_6$)$_2$** can be obtained from 1,1′-fc[B(Me)Br]$_2$ [**2**; fc: $(C_5H_4)_2Fe$], two equiv. of ligand **C** and an excess of NH_4PF_6.

Attempts to synthesise dinuclear **[1C1]Br$_2$** either from two equiv. of **1** and one equiv. of **C** or from equal amounts of **1** and **[1C]Br** generated a deep brown solid product. ^{1}H NMR spectroscopy ([D$_6$]DMSO) and a FAB-MS (*m*/*z* = 735, {**[1C1]Br**}$^+$) provided some evidence that the reaction product contained **[1C1]Br$_2$**. The complex is highly air- and moisture-sensitive and poorly soluble in all common solvents. An analytically pure sample was not obtained. **[1C1]Br$_2$** slowly decomposed in [D$_6$]DMSO (dried over molecular sieves for a period of several days) to give **[1C]Br** and free ferrocene as the major products. Thus, **[1C1]Br$_2$** appears to be considerably more fragile than **[1C]Br**, which is even stable to water (see above). This finding might be explained by the sharp decrease in the basicity of the second pyrazine nitrogen atom in bppz upon coordination of the first nitrogen centre (*cf.* parent pyrazine: pK_a(1) = 0.65, pK_a(2) = −5.78; in water, 27 °C).[16] Since this effect is much less pronounced in 4,4′-bipyridine (pK_a(1) = 4.82, pK_a(2) = 3.17; in water, 25 °C),[17] ligand **D** was employed in the further attempts to generate stable dinuclear complexes. Indeed, the green water- and air-stable **[1D1]Br$_2$** has been obtained in almost quantitative yield by the reaction of **D** with two equiv. of **1** in CH_2Cl_2.

[2D]$_2$Br$_4$ was synthesised in high yield from **2** and 1 equiv. of **D** in CH_2Cl_2. Due to the poor solubility of the compound in water, the salt metathesis reaction was this time performed with $TlPF_6$ in CH_3CN. The resulting **[2D]$_2$(PF$_6$)$_4$** is air- and water-stable and possesses a good solubility in polar solvents such as acetonitrile or dimethyl sulfoxide.

NMR Spectroscopy

The ^{11}B NMR spectrum of **[1C]PF$_6$** shows a broad signal at δ 7.5, which lies in a range typical of tetra-coordinate boron nuclei.[18] In the ^{1}H NMR spectrum, the four protons of the substituted cyclopentadienyl ring show four different resonances. This feature, which does not change when the spectrum is run at elevated temperature, indicates the boron atom to be a chiral centre. The free ligand **C** presents five signals,[14] while the bppz fragment of **[1C]PF$_6$** gives rise to ten proton resonances, which can be divided into two subsets possessing equal intensity. One subset is similar to the proton spectrum of **C**, while the signals of the other appear at lower field. Most chemical shifts of the second subset are close to those of the coordinated 2,2′-bipyridine ligand in **B1**.[12] From an inspection of the integral values in the ^{1}H NMR spectrum of **[1C]PF$_6$**, it is apparent, that the ratio between ferrocene and the bppz unit is 1 : 1. The same general signal pattern as in the ^{1}H NMR spectrum of **[1C]PF$_6$** is found in its ^{13}C NMR spectrum, which exhibits fourteen rather than seven resonances for the bppz moiety. A common feature of carbon atoms attached to boryl substituents is an extreme broadening of their ^{13}C NMR resonances.[18] Consequently, the methyl group in **[1C]PF$_6$** appears as a broad hump, and the C_5H_4-*ipso* atom of the ferrocene subunit could not be detected at all.

The ^{11}B, ^{1}H and ^{13}C NMR data of **[2C$_2$](PF$_6$)$_2$** show similar characteristics as in the case of **[1C]PF$_6$**. However, both the ^{1}H and the ^{13}C NMR spectra indicate **[2C$_2$](PF$_6$)$_2$** to exist as a mixture of two isomers (ratio 3 : 4). Since **[2C$_2$](PF$_6$)$_2$** possesses two chiral boron atoms, the two isomers are most likely diastereomers with *meso* and *rac* configuration.

The ^{11}B NMR resonance of **[1D1](PF$_6$)$_2$** at δ 11.8 is characteristic of tetra-coordinate boron nuclei.[18] The qpy moiety gives rise to only one set of signals both in the ^{1}H and in the ^{13}C NMR spectrum, indicating a high symmetry of the molecular framework. The substituted cyclopentadienyl rings exhibit four proton and four carbon resonances, which can again be attributed to the influence of the chiral boron substituents. NMR spectroscopy further indicates, that either the formation of **[1D1](PF$_6$)$_2$** is diastereoselective, or the two possible diastereomers possess the same chemical shift values. The ESI mass spectrum of the bromide salt **[1D1]Br$_2$** shows peaks of the monocation {**[1D1]Br**}$^+$ (*m*/*z* = 811) and the dication **[1D]**$^{2+}$ (*m*/*z* = 366).

The NMR spectra of **[2D]$_2$(PF$_6$)$_4$** are very similar to those of the related compound **[1D1](PF$_6$)$_2$**. ^{11}B NMR spectroscopy [δ(^{11}B) = 12.4] again clearly reveals the presence of tetra-coordinate boron centres,[18] which, according to the proton resonance pattern of the C_5H_4-rings [δ(^{1}H) = 4.22, 4.17, 4.12, 3.74], possess a chiral configuration. The ^{1}H NMR spectrum, as well as the ^{13}C NMR spectrum, testifies to the high average symmetry of the molecule in solution. In the case of **[1D1](PF$_6$)$_2$**, the borylated cyclopentadienyl ring gives rise to four well-resolved ^{13}C NMR signals. In contrast, one extremely broad hump was detected in the ferrocene region of the ^{13}C NMR spectrum of **[2D]$_2$(PF$_6$)$_4$**. Upon cooling to *T* = 243 K, this signal splits into two resonances (δ 70.3, 68.7; CD_3CN), which are still rather broad. A comparison with the ^{13}C NMR signal pattern of the ferrocenyl moieties of **[1D1](PF$_6$)$_2$** suggests, that the two signals of **[2D]$_2$(PF$_6$)$_4$** have to be addressed as an incompletely resolved set of four resonances. Two ^{13}C NMR signals in the ferrocene region are also observed when the sample is heated to *T* = 323 K (δ 70.5, 68.8; CD_3CN). These observations point towards some fluxionality in the molecule, which is moderate at ambient temperature on the NMR timescale. NMR signals of minor intensity, which could be attributed to the chain ends of oligomeric species, have not been detected. ESI mass spectrometry, a particularly mild tool for the investigation even of fragile oligomeric compounds, shows two dominant peaks at *m*/*z* = 691 and 412, which can be assigned to the ions {**[2D]$_2$(PF$_6$)$_2$**}$^{2+}$ and {**[2D]$_2$(PF$_6$)**}$^{3+}$, respectively. No fragments of higher masses were observed.

Gel permeation chromatography

GPC measurements have been performed (i) to make sure that the reaction outlined in Scheme 2 yielded one product only, and (ii) to determine the size of the molecules obtained. Mass spectrometry already gave some evidence for the formation of macrocycles **[2D]$_2^{4+}$**. Given this background, we included the dinuclear compound **[1D1](PF$_6$)$_2$** into our GPC measurements. If the macrocyclic structure proposed for **[2D]$_2$(PF$_6$)$_4$** is correct, the two compounds would have approximately the same size and can thus be expected to show similar retention times on the GPC column.

In a first series of measurements, acetonitrile solutions of **[1D1](PF$_6$)$_2$** on one hand and **[2D]$_2$(PF$_6$)$_4$** on the other have been investigated [stationary phase: PLgel 100A, 5 μm, (300 × 7.5) mm]. Each of the compounds showed only one peak with a retention time of 8.08 min {**[1D1](PF$_6$)$_2$**} and 8.03 min {**[2D]$_2$(PF$_6$)$_4$**}. In both cases there was no evidence for the presence of any byproducts possessing higher molecular weights. In a second experiment, a GPC analysis of an equimolar mixture of **[1D1](PF$_6$)$_2$** and **[2D]$_2$(PF$_6$)$_4$** in acetonitrile was performed ("spiking"), which gave one single peak with a retention time of 8.13 min.

Gel permeation chromatography thus strongly supports our previous conclusion, that (i) the reaction of **2** with one equiv. of quaterpyridine is very selective and (ii) the product obtained consists of cyclic dimers **[2D]$_2$(PF$_6$)$_4$** rather than chain-like polymers.

X-Ray crystal structure analyses

Gas phase diffusion of diethyl ether into an acetonitrile solution of **[2C$_2$](PF$_6$)$_2$** afforded X-ray quality crystals. Details of the X-ray crystal structure analysis are summarised in Table 1.

As has been deduced from the NMR spectra, **[2C$_2$](PF$_6$)$_2$** features two chiral tetra-coordinate boron atoms (Fig. 2), each of them possessing a distorted tetrahedral geometry with angles N(21)–B(1)–N(31) and N(61)–B(2)–N(71) of 94.3(4) and 93.8(4)°, respectively (Table 2).

Table 1 Crystal data and structure refinement details of $[2C_2](PF_6)_2$

	$[2C_2](PF_6)_2$
Formula	$C_{40}H_{34}B_2F_{12}FeN_8P_2$
M_w/g mol^{-1}	994.16
Crystal dimensions/mm	0.90 × 0.50 × 0.30
Crystal system	Triclinic
Space group	$P\bar{1}$ (no.2)
T/K	293 ± 2
a/Å	12.973(5)
b/Å	14.478(5)
c/Å	15.575(5)
α/°	109.470(5)
β/°	94.120(5)
γ/°	113.171(5)
V/Å^3	2465.1(15)
D_c/g cm^{-3}	1.339
Z	2
Radiation, λ/Å	Mo-Kα, 0.71073
No. of total reflns.	26884
No. of unique reflns.	10943
No. of parameters	586
μ/cm^{-1}	4.53
Final $R1$ (all data)[a]	0.1582
Final $wR2$ (all data)[b]	0.2589
GOF[c]	0.864

[a] $R1 = \Sigma(||F_o| - |F_c||)/\Sigma|F_o|$. [b] $wR2 = [\Sigma w(F_o^2 - F_c^2)^2/\Sigma w(F_o^2)^2$. [c] GOF = $[\Sigma w(F_o^2 - F_c^2)^2/(N_o - N_v)]^{1/2}$; N_o = no. of observations, N_v = no. of variables.

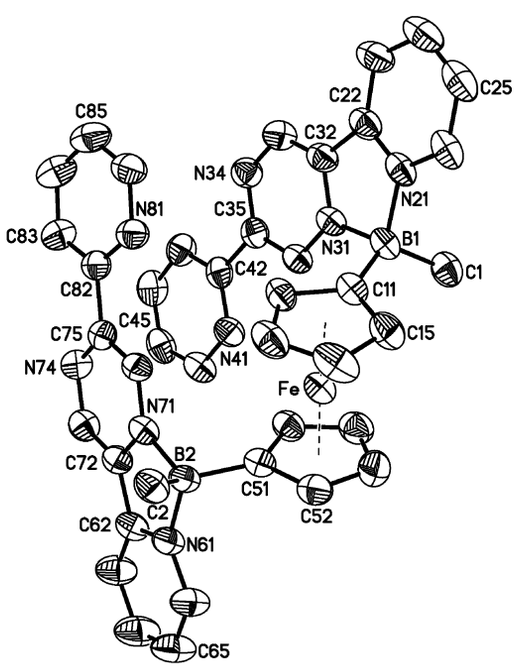

Fig. 2 Molecular structure of $[2C_2](PF_6)_2$ in the solid state; hydrogen atoms and $[PF_6]^-$ ions have been omitted for clarity.

The single crystal under investigation here consisted of the *rac* diastereomer only. The bond lengths between boron and the two nitrogen atoms of the bppz ligand are almost equal within experimental error in both Bbppz units [B(1)–N(21) 1.616(7), B(1)–N(31) 1.598(7); B(2)–N(61) 1.610(7), B(2)–N(71) 1.608(7)]. The angle between the vectors C(42) ··· C(45) of the non-coordinating pyridyl substituent and C(32) ··· C(35) of the pyrazyl ring is 3.7° [angle between C(82) ··· C(85) and C(72) ··· C(75): 4.4°]. In contrast, an angle of 20.6° is found between the vectors C(22) ··· C(25) of the coordinating pyridyl substituent and C(32) ··· C(35) [angle between C(62) ··· C(65) and C(72) ··· C(75): 20.1°]. Chelation of the small boron centre thus leads to a substantial bending of the bppz framework. This observation helps to explain the low stability of the dinuclear complex $[1C1]Br_2$, since coordination of a second boron atom to **[1C]Br** can be expected to cause a severe further increase in ligand strain.

Table 2 Selected bond lengths (Å), bond angles and torsion angles (°) of $[2C_2](PF_6)_2$

B(1)–C(1)	1.586(9) [1.600(7)][a]
B(1)–C(11)	1.583(7) [1.581(8)]
B(1)–N(21)	1.616(7) [1.610(7)]
B(1)–N(31)	1.598(7) [1.608(7)]
N(21)–C(22)	1.361(7) [1.359(7)]
N(31)–C(32)	1.349(7) [1.350(6)]
C(22)–C(32)	1.463(7) [1.450(7)]
N(21)–B(1)–N(31)	94.3(4) [93.8(4)]
N(21)–B(1)–C(1)	108.5(4) [111.0(4)]
N(31)–B(1)–C(1)	111.2(4) [111.7(5)]
N(21)–B(1)–C(11)	111.9(4) [108.2(4)]
N(31)–B(1)–C(11)	109.2(4) [111.7(5)]
C(1)–B(1)–C(11)	118.9(5) [119.9(4)]
B(1)–N(21)–C(22)	113.0(4) [113.8(4)]
B(1)–N(31)–C(32)	114.1(4) [113.6(4)]
N(21)–C(22)–C(32)	109.1(5) [108.8(4)]
N(31)–C(32)–C(22)	109.4(5) [110.0(4)]
N(34)–C(35)–C(42)	118.7(5) [116.9(4)]
N(41)–C(42)–C(35)	114.9(5) [114.5(4)]
C(23)–C(22)–C(32)	129.9(6) [129.4(5)]
C(33)–C(32)–C(22)	131.9(5) [130.7(5)]
C(36)–C(35)–C(42)	119.6(5) [120.7(4)]
C(43)–C(42)–C(35)	122.1(5) [122.5(5)]
C(1)–B(1)–C(11)–C(12)	−145.9(5) [40.9(8)]
C(23)–C(22)–C(32)–C(33)	−2.4(10) [0.3(10)]
C(36)–C(35)–C(42)–N(41)	1.7(7) [6.4(5)]

[a] Numbers in parentheses refer to the corresponding bond lengths and angles of the second B(Me)bppz substituent.

While the related bipy derivative **B2** (Fig. 1) adopts a sterically favourable transoid conformation in the solid state,[12] $[2C_2](PF_6)_2$ presents a geometry which results in close contacts between the aromatic moieties of its two B(Me)bppz substituents (distance between COG[N(41) to C(46)] and COG[N(71) to C(76)]: 3.9 Å; distance between COG[N(81) to C(86)] and COG[N(31) to C(36)]: 4.2 Å; COG: centre of gravity). This feature might be caused by an intramolecular charge transfer (CT) between the non-coordinating pyridines and the electron-deficient pyrazines.

The crystal and molecular structures of two pseudopolymorphs of $[1C]PF_6$ have been determined by us and were published elsewhere.[19] All bond lengths and angles are rather similar to those of $[2C_2](PF_6)_2$.

So far, all attempts to grow single crystals of $[2D]_2(PF_6)_4$ have not met with success. It therefore still remains unclear whether it consists of isomer 1, isomer 2, or a mixture of both. However, investigations of related macrocycles containing 2,5-bis-(pyrazol-1-yl)benzoquinone rather than qpy as a bridging unit suggest isomer 1 of $[2D]_2(PF_6)_4$ to possess the most favourable molecular structure.[20]

Electrochemical investigations

Fig. 3 shows the cyclic voltammetric behaviour of the mono- and di-substituted ferrocenes $[1C]PF_6$ and $[2C_2](PF_6)_2$ in *N*,*N*-dimethylformamide solution.

The monocation $[1C]^+$ gives rise to one ferrocenyl-centred oxidation and two bppz-centred reductions. All these processes display features of chemical reversibility on the cyclic voltammetric timescale. Controlled potential coulometric tests performed in correspondence with the anodic step (E_w = +0.8 V) consume one electron per molecule. Upon exhaustive oxidation the original deep green solution (λ_{max} = 600 nm) turns light green (λ_{max} = 625 nm) and displays a cyclic voltammetric profile complementary to the original one. These data indicate a high stability of the Fe(III) dication $[1C]^{2+}$ in solution. An analysis of

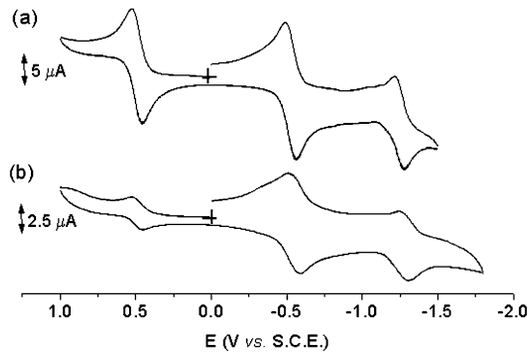

Fig. 3 Cyclic voltammograms recorded at a platinum electrode in DMF solutions containing $[NEt_4]PF_6$ (0.1 mol dm^{-3}) and (a) **[1C]PF$_6$** (1.3×10^{-3} mol dm^{-3}), (b) **[2C$_2$](PF$_6$)$_2$** (0.3×10^{-3} mol dm^{-3}): scan rate 0.2 V s^{-1}.

the cyclic voltammograms with scan rates varying from 0.02 to 1.00 V s^{-1} not only confirms the chemical reversibility of the one-electron oxidation (i_{pc}/i_{pa} constantly equal to 1), but also proves its electrochemical reversibility (ΔE_p constantly close to 60 mV), thereby suggesting no significant structural reorganization to occur upon electron removal. The first reduction step was found to be also chemically reversible on the electrolysis timescale ($E_w = -0.7$ V). In the UV-vis spectrum, the electrogenerated olive-green radical species **[1C]^0** displayed a flattened band at $\lambda_{max} = 725$ nm. Given the chemical reversibility of the redox sequence **[1C]$^{2+/+/0}$**, the slightly lower peak-height of the second cathodic step is attributed to weak electrode poisoning effects (it is noted that in dichloromethane solution no such effect is detected).

The cyclic voltammetric profile of **[2C$_2$]$^{2+}$** is conceivably attributed to the one-electron oxidation of the ferrocenediyl core and to the concomitant one-electron reductions of the two bppz ligands. The latter result in two single two-electron processes. Again in this case, the peak-height of the most cathodic step appears to be affected by electrode poisoning phenomena. At variance with **[1C]$^{+/0}$**, the first (two-electron) reduction is accompanied by chemical complications, as indicated by the fact, that the i_{pa}/i_{pc} ratio progressively increases with increasing scan rates from a value of 0.5 at 0.02 V s^{-1} to 0.8 at 1.00 V s^{-1}. Unfortunately, in this case the use of dichloromethane afforded even more severe and extended electrode adsorption phenomena. The fact that the two bppz ligands are reduced at the same electrode potentials testifies to the fact that no electronic interaction exists between them.

An interesting redox behaviour is displayed by complex **[1D1]$^{2+}$** (Fig. 4). The compound exhibits a single two-electron

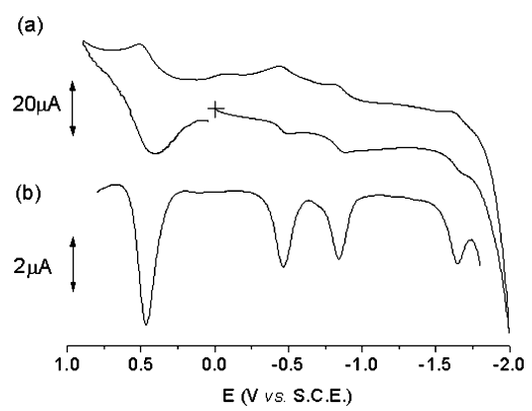

Fig. 4 Cyclic (a) and differential pulse (b) voltammograms recorded at a platinum electrode on a DMF solution containing $[NEt_4]PF_6$ (0.1 mol dm^{-3}) and **[1D1](PF$_6$)$_2$** (0.3×10^{-3} mol dm^{-3}). Scan rates: (a) 0.2 V s^{-1}. (b) 0.02 V s^{-1}.

oxidation (coulometric control), which can be assigned to the simultaneous oxidation of the two terminal ferrocenyl substituents, as well as three sequential one-electron reductions centred on the quaterpyridine spacer. A fourth reduction step might be obscured by the solvent discharge. It is interesting that the first of the **[1D1]$^{2+}$** reduction steps ($E^{o\prime} = -0.49$ V) occurs at a potential less negative by 0.53 V with respect to the related monocation **B1** ($E^{o\prime} = -1.02$ V; Table 3).[12] This can be attributed in part to electrostatic effects, but the more extended π conjugated system of the quaterpyridine linker certainly plays an important additional role.

The macrocyclic complex **[2D]$_2$[PF$_6$]$_4$** gives a voltammetric pattern substantially similar to that of **[1D1]$^{2+}$** (Fig. 5).

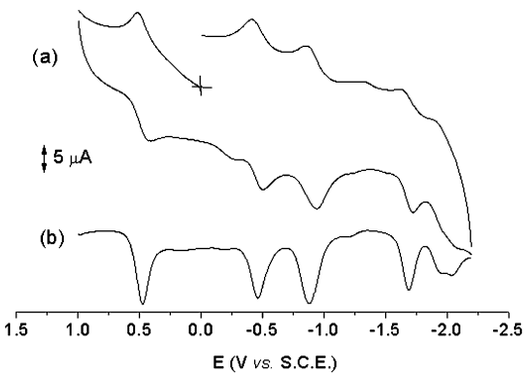

Fig. 5 Cyclic (a) and differential pulse (b) voltammograms recorded at a platinum electrode on a DMF solution containing $[NEt_4]PF_6$ (0.1 mol dm^{-3}) and **[2D]$_2$(PF$_6$)$_4$** (0.3×10^{-3} mol dm^{-3}). Scan rates: (a) 0.2 V s^{-1}, (b) 0.02 V s^{-1}.

However, an important difference lies in the better defined four-step reduction sequence exhibited by **[2D]$_2$[PF$_6$]$_4$**. It should be pointed out, that the first ferrocene-centred oxidation substantially displays the same peak-height as each of the reduction steps. Controlled potential coulometry in correspondence with the first oxidation process ($E_w = +0.6$ V) consumed about 2.1 electrons, thus suggesting all the processes to be two-electron steps. These results are in good agreement with the proposed macrocyclic structure of **[2D]$_2$[PF$_6$]$_4$**, as it has been deduced from NMR, ESI-MS and GPC data. Also in this case, any electronic communication remains confined inside the quaterpyridine spacer and does not overcome the ferrocene barrier. All electrode potentials of the redox changes discussed below are compiled in Table 3.

Conclusion

The potential of the difunctional chelating amines bppz (**C**, Fig. 1) and qpy (**D**, Fig. 1) for the generation of stable oligomeric ferrocenylborane aggregates has been evaluated. It has been shown, that the pyrazine derivative bppz is not a suitable bridging element for the connection of two boron centres. This is partly due to the fact, that the Lewis basicity of the second binding site drops sharply upon coordination of the first boron centre. Moreover, chelation of the small boron atom causes a distortion of the bppz framework thereby disfavouring its coordination to a second boron atom. In contrast, the 4,4′-bipyridine derivative qpy is able to form very stable adducts to two boron atoms at the same time. The reaction of the diborylated ferrocene **2** with qpy selectively leads to the macrocyclic dimer **[2D]$_2$[PF$_6$]$_4$** rather than to polymeric material. The opposite is true for the reaction of 1,1′-fc(BMe$_2$)$_2$ with parent 4,4′-bipyridine or pyrazine [fc = $(C_5H_4)_2Fe$], which has been shown to give polymeric chains *via* B–N adduct formation in the solid state.

Table 3 Formal electrode potentials (V *vs.* SCE) and peak-to-peak separations (mV) for the redox changes exhibited by complexes **[1C]PF$_6$**, **[2C$_2$](PF$_6$)$_2$**, **[1D1](PF$_6$)$_2$** and **[2D]$_2$(PF$_6$)$_4$** in different solvents

	Fc-centred oxidation		Ligand-centred reductions								
	$E^{\circ\prime}$/V	ΔE_p[a]/mV	$E^{\circ\prime}$/V	ΔE_p[a]/mV	$E^{\circ\prime}$/V	ΔE_p[a]/mV	$E^{\circ\prime}$/V	ΔE_p[a]/mV	$E^{\circ\prime}$/V	ΔE_p[a]/mV	Solvent
[1C]$^+$	+0.50	58	−0.52	59	−1.25	53					DMF[b]
	+0.47	65	−0.59	61	−1.41	57					CH_2Cl_2[b]
[2C$_2$]$^{2+}$	+0.48	63	−0.56[c]	80	−1.28[c]	54					DMF[b]
	+0.51	178	−0.62[c]	42	−1.39[c]	66					CH_2Cl_2[b]
[1D1]$^{2+}$	+0.48[c]	63	−0.49	75	−0.87	57	−1.64[d]	—	—[e]	—	DMF[b]
	+0.40[c]	70	−0.51	65	−0.99	60	—[f]	—	[e]	—	CH_2Cl_2[b]
B1	+0.40	64			−1.02	64			−1.71	66	DMF[b]
	+0.42	66			−0.99	70			−1.79[g]	—	CH_2Cl_2[b]
[2D]$_2^{4+}$	+0.47[c]	65	−0.46[c]	55	−0.87	103[c]	−1.64[c]	106	−1.97[d]		DMF[b]
	+0.38[c]	70	−0.52[c]	54	−0.98	103[c]	−1.69[c,h]	80[h]	—		CH_2Cl_2[b]
FcH	+0.49	60									DMF[b]
	+0.39	82									CH_2Cl_2[b]

[a] Measured at 0.1 V s^{-1}. [b] [NBu$_4$]PF$_6$ (0.2 mol dm^{-3}) supporting electrolyte. [c] Two-electron process. [d] From DPV. [e] Not detected. [f] Difficult to detect. [g] Irreversible process. [h] Measured at 1.0 V s^{-1}.

Experimental

General considerations

All reactions and manipulations of air-sensitive compounds were carried out in dry, oxygen-free argon using standard Schlenk ware. Solvents were freshly distilled under N_2 from Na/K alloy–benzophenone (toluene, hexane) or from CaH_2 (CH_2Cl_2, CH_3CN) prior to use. NMR: JEOL JMN–GX 400, Bruker AMX 250, Bruker DPX 250 spectrometers. ^{11}B NMR spectra are reported relative to external $BF_3{\cdot}Et_2O$. Unless stated otherwise, all NMR spectra were run at ambient temperature. Abbreviations: s = singlet; d = doublet; t = triplet; vtr = virtual triplet; dd = doublet of doublets; ddd = doublet of doublets of doublets; br = broad; m = multiplet; n.r. = multiplet expected in the ^{1}H NMR spectrum but not resolved; n.o. = signal not observed, pyridine = py, pyrazine = pyz, quaterpyridine = qpy. NMR spectra of **[1C]PF$_6$** and **[2C$_2$](PF$_6$)$_2$**: signals marked with an (′) belong to those rings of the bppz ligand, which are coordinated to boron. Elemental analyses: Microanalytical laboratory of the Frankfurt University. The compounds **1**,[10,11] **2**,[10,11] 2,5-bis-(pyridyl)pyrazine (**C**)[14] and quaterpyridine (**D**)[15] were synthesised according to literature procedures.

Synthesis of [1C]PF$_6$

A toluene (10 mL) solution of **1** (0.29 g, 1.00 mmol) was added dropwise with stirring at room temperature to a solution of 2,5-bis(pyridyl)pyrazine (**C**) (0.23g, 0.98 mmol) in 60 mL of toluene. The mixture instantaneously adopted a green–blue colour, and a blue precipitate formed immediately. The slurry was stirred for 3 h, and the light yellow solution was removed using a filter cannula. The green–blue solid residue (**[1C]Br**) was triturated with hexane (3 × 20 mL) and dried *in vacuo*. **[1C]Br** was dissolved in 150 mL of water, and the clear green solution was added dropwise at room temperature to an aqueous solution of NH_4PF_6 (0.33 g, 2.02 mmol), whereupon **[1C]PF$_6$** precipitated quantitatively. Yield: 0.51 g (88%).

^{11}B NMR (128.3 MHz, $CDCl_3$): δ 7.5 ($h_{1/2}$ = 1440 Hz). ^{1}H NMR (400.0 MHz, [D$_8$]THF): δ 10.21, 10.13 (2 × s, 2 × 1H; pyz-3,6), 9.08 (d, 1H, ^3J(HH) = 7.7 Hz; py-6′), 9.02 (d, 1H, ^3J(HH) = 5.5 Hz; py-3′), 8.82 (d, 1H, ^3J(HH) = 4.8 Hz; py-6), 8.71 (m, 2H; py-3,4′), 8.14 (dd, 1H, ^3J(HH) = 7.7 and 5.5 Hz; py-5′), 8.08 (vtr, 1H, ^3J(HH) = 7.7 Hz; py-4), 7.61 (dd, 1H, ^3J(HH) = 7.7 and 4.8 Hz; py-5), 4.30 (s, 5H; C_5H_5), 4.29, 4.18, 4.15, 3.69 (4 × n.r., 4 × 1H; C_5H_4), 0.78 (s, 3H; CH_3). ^{13}C NMR (62.9 MHz, [D$_6$]DMSO): δ 154.8 (py-2), 150.9 (pyz-5), 150.3 (py-6), 145.6 (pyz-3 or 6), 144.4 (py-4′), 143.6 (py-6′), 143.0 (py-2′), 138.5 (pyz-2), 138.4 (py-4), 133.2 (pyz-3 or 6), 128.9 (py-5′), 126.9 (py-5), 123.8 (py-3′), 122.5 (py-3), 71.0, 70.0, 69.6, 69.3 (C_5H_4), 68.2 (C_5H_5), 7.7 (CH_3), n.o. (C_5H_4-*ipso*). The assignments were done with the aid of a C,H–COSY NMR spectrum. Note: The proton chemical shifts are strongly dependent on the nature of the solvent. FAB–MS: *m*/*z* = 445 [(M − PF$_6$)$^+$; 100%]. Anal. Calc. for $C_{25}H_{22}BF_6FeN_4P$ (590.11): C, 50.89; H, 3.76; N, 9.50. Found: C, 50.92; H, 3.93; N, 9.27%.

Synthesis of [2C$_2$](PF$_6$)$_2$

A toluene (10 mL) solution of **2** (0.11 g, 0.28 mmol) was added with stirring at −60 °C to a solution of 2,5-bis(pyridyl)pyrazine (**C**) (0.13 g, 0.55 mmol) in 75 mL of toluene. The mixture instantaneously adopted a green colour. Upon warming to ambient temperature, a precipitate gradually formed. The slurry was stirred for 3 h, insoluble material (**[2C$_2$]Br$_2$**) was isolated by filtration, treated with hexane (30 mL) and dried *in vacuo*. **[2C$_2$]Br$_2$** was dissolved in 50 mL of water, and the clear green solution was added dropwise at room temperature to an aqueous solution of NH_4PF_6 (0.18 g, 1.10 mmol), whereupon **[2C$_2$](PF$_6$)$_2$** precipitated quantitatively. Yield: 0.18 g (66%). Green X-ray-quality crystals were grown by gas phase diffusion of diethyl ether into an acetonitrile solution of **[2C$_2$](PF$_6$)$_2$**.

^{11}B NMR (128.3 MHz, [D$_6$]DMSO): δ 5.7 ($h_{1/2}$ = 2100 Hz). ^{1}H NMR (250.1 MHz, [D$_6$]DMSO): *meso*-compd.: δ 10.44, 9.86 (2 × s, 2 × 2H, pyz-3,6), 9.14 (m, 4H, py-3′,6′), 8.79 (m, 2H, py-6), 8.71 (vtr, 2H, ^3J(HH) = 7.6 Hz, py-4′), 8.59 (d, 2H, ^3J(HH) = 7.9 Hz, py-3), 8.22 (vtr, 2H, ^3J(HH) = 7.6 Hz, py-5′), 8.09 (vtr, 2H, ^3J(HH) = 7.9 Hz, py-4), 7.72 (dd, 2H, ^3J(HH) = 7.9 and 5.5 Hz, py-5), 4.34, 4.15, 4.03 (3 × n.r., 4H, 2 × 2H, C_5H_4), 0.63 (s, 6H, CH_3). *rac*-compd.: 10.32, 9.82 (2 × s, 2 × 2H, pyz-3,6), 9.14 (m, 4H, py-3′,6′), 8.79 (m, 2H, py-4′), 8.48 (d, 2H, ^3J(HH) = 5.5 Hz, py-6), 8.23 (m, 6H, py-3,4,5′), 7.62 (dd, 2H, ^3J(HH) = 6.8 and 5.5 Hz, py-5), 4.62, 4.57, 4.37, 3.98 (4 × n.r., 4 × 2H, C_5H_4), 0.68 (s, 6H, CH_3). ^{13}C NMR (62.9 MHz, [D$_6$]DMSO): *meso*-compd.: δ 154.8 (py-2), 150.8 (pyz-5), 150.2 (py-6), 145.7 (pyz-3 or 6), 144.4 (py-4′), 143.6 (py-6′), 143.0 (py-2′), 138.5 (pyz-2), 138.3 (py-4), 133.1 (pyz-3 or 6), 128.9 (py-5′), 126.9 (py-5), 123.7 (py-3′), 122.6 (py-3), 83.0 (C_5H_4-*ipso*), 70.9, 70.4, 70.1, 69.9 (C_5H_4), 7.2 (CH_3). *rac*-compd.: 154.1 (py-2), 150.2 (pyz-5), 149.9 (py-6), 145.3 (pyz-3 or 6), 144.2 (py-4′), 143.4 (py-6′), 142.7 (py-2′), 138.4 (pyz-2), 138.4 (py-4), 133.0 (pyz-3 or 6), 129.1 (py-5′), 126.8 (py-5), 124.1 (py-3′), 122.2 (py-3), 83.0 (C_5H_4-*ipso*), 71.8, 71.1, 70.5, 69.9 (C_5H_4), 7.2 (CH_3). Anal. Calc. for $C_{40}H_{34}B_2F_{12}FeN_8P_2$ (994.16) + H_2O (18.00): C, 47.47; H, 3.59; N, 11.07. Found: C, 47.80; H, 3.92; N, 10.86%. Ratio: *meso* : *rac* is about 3 : 4.

Synthesis of [1C1]Br$_2$

Method 1. A toluene (2 mL) solution of **1** (0.07 g, 0.24 mmol) was added dropwise with stirring at room temperature to a

CH_2Cl_2 (40 mL) solution of **[1C]Br** (0.13 g, 0.25 mmol). A brown precipitate slowly formed, the resulting slurry was stirred for 1.5 h, filtered off, and the solid residue was dried *in vacuo*. Yield: 0.19 g (97%).

Method 2. A toluene (100 mL) solution of **C** (0.20 g, 0.85 mmol) was added dropwise with stirring at room temperature to a solution of **1** (0.51 g, 1.75 mmol) in toluene (10 mL). A red brown solid precipitated immediately, the resulting slurry was stirred for 1.5 h, filtered off, and the residue was dried *in vacuo*. Yield: 0.58 g (84%).

Synthesis of [1D1](PF$_6$)$_2$

A CH_2Cl_2 (20 mL) solution of **1** (0.29 g, 1.00 mmol) was slowly added with stirring at −78 °C to a solution of quaterpyridine (**D**) (0.15 g, 0.48 mmol) in 10 mL of CH_2Cl_2. The reaction mixture instantaneously adopted a deep green colour. The solution was allowed to warm to ambient temperature and stirred for 2 days. After a small amount of insoluble material had been removed by filtration, the filtrate was treated with 30 mL of hexane, whereupon a green microcrystalline solid precipitated (**[1D1]Br$_2$**), which was washed with hexane (2 × 20 mL) and dried *in vacuo*. **[1D1]Br$_2$** was dissolved in 50 mL of water, and the clear purple solution was added dropwise at room temperature to an aqueous solution of NH_4PF_6 (0.33 g, 2.02 mmol), whereupon **[1D1](PF$_6$)$_2$** precipitated quantitatively. Yield: 0.45 g (92%).

^{11}B NMR (128.3 MHz, CD_3CN): δ 11.8 ($h_{1/2}$ = 390 Hz). ^{1}H NMR (250.0 MHz, CD_3CN): δ 9.20 (dd, 2H, ^3J(HH) = 6.1 Hz, ^5J(HH) = 0.6 Hz, qpy-6′,6″), 9.14 (dd, 2H, ^4J(HH) = 1.8 Hz, ^5J(HH) = 0.6 Hz, qpy-3′,3″), 9.07 (ddd, 2H, ^3J(HH) = 5.7 Hz, ^4J(HH) = ^5J(HH) = 1.3 Hz, qpy-6,6‴), 8.80 (ddd, 2H, ^3J(HH) = 7.6 Hz, ^4J(HH) = ^5J(HH) = 1.3 Hz, qpy-3,3‴), 8.69 (ddd, 2H, ^3J(HH) = 7.6 Hz and 7.6 Hz, ^4J(HH) = 1.3 Hz, qpy-4,4‴), 8.54 (dd, 2H, ^3J(HH) = 6.1 Hz, ^4J(HH) = 1.8 Hz, qpy-5′,5″), 8.19 (ddd, 2H, ^3J(HH) = 7.6 Hz and 5.7 Hz, ^4J(HH) = 1.3 Hz, qpy-5,5‴), 4.26, 4.24, 3.94, 3.80 (4 × m, 4 × 2H, C_5H_4), 4.13 (s, 10H, C_5H_5), 0.71 (s, 6H, CH_3). ^{13}C NMR (62.9 MHz, CD_3CN): δ 150.8, 147.2, 145.7 (qpy-2,2′,2″,2‴,4′,4″), 145.7 (qpy-4,4‴), 145.1 (qpy-6′,6″), 144.6 (qpy-6,6‴), 130.2 (qpy-5,5‴), 128.1 (qpy-5′,5″), 124.2 (qpy-3,3‴), 122.9 (qpy-3′,3″), 71.1, 71.0, 70.9, 70.8 (C_5H_4), 69.3 (C_5H_5), n.o. (C_5H_4-*ipso* and BCH_3). Anal. Calc. for $C_{42}H_{38}B_2F_{12}Fe_2N_4P_2$ (1022.03): C, 49.36; H, 3.75; N, 5.48. Found: C, 49.02; H, 4.12; N, 5.27%. The assignments were done with the aid of a C,H–COSY NMR spectrum. ESI-MS of **[1D1]Br$_2$**: *m*/*z* 811 [(M − Br)$^+$; 72%], 366 [(M − 2Br)$^{2+}$; 100%].

Synthesis of [2D]$_2$(PF$_6$)$_4$

A CH_2Cl_2 (80 mL) solution of **2** (0.34 g, 0.86 mmol) was slowly added with stirring at −78 °C to a solution of quaterpyridine (**D**) (0.27 g, 0.87 mmol) in 20 mL of CH_2Cl_2. The reaction mixture instantaneously adopted a green colour, and a green precipitate gradually formed upon warming to ambient temperature. After stirring for 2 days at ambient temperature, the green insoluble solid **[2D]$_2$Br$_4$** was collected on a frit, extracted with CH_2Cl_2 (2 × 10 mL) and dried *in vacuo*. $TlPF_6$ (0.50 g, 1.43 mmol) in CH_3CN (15 mL) was added to a slurry of **[2D]$_2$Br$_4$** (0.51 g, 0.36 mmol) in 20 mL of CH_3CN at ambient temperature with stirring, whereupon the colour of the supernatant changed from colourless to deep blue. After stirring for 12 h, the insoluble white precipitate of TlBr was removed by filtration, and the filtrate was dried *in vacuo*. **[2D]$_2$(PF$_6$)$_4$** was obtained as a deep blue microcrystalline solid. Yield: 0.60 g (83%).

^{11}B NMR (128.3 MHz, CD_3CN): δ 12.4 ($h_{1/2}$ = 1500 Hz). ^{1}H NMR (250.0 MHz, CD_3CN): δ 9.16 (m, 8H, qpy-6′,6″ and qpy-3′,3″), 9.02 (d, 4H, ^3J(HH) = 5.3 Hz, qpy-6,6‴), 8.82 (d, 4H, ^3J(HH) = 7.9 Hz, qpy-3,3‴), 8.69 (vtr, 4H, qpy-4,4‴), 8.55 (d, 4H, ^3J(HH) = 6.1 Hz, qpy-5′,5″), 8.18 (m, 4H, qpy-5,5‴), 4.22, 4.17, 4.12, 3.74 (s, 4 × 2H, C_5H_4), 0.70 (s, 12H, CH_3). ^{13}C NMR (62.9 MHz, 243 K, CD_3CN): δ 150.0, 146.6, 145.2 (qpy-2,2′,2″,2‴,4′,4″), 145.1 (qpy-4,4‴), 144.4 (qpy-6′,6″), 143.9 (qpy-6,6‴), 129.6 (qpy-5,5‴), 127.5 (qpy-5′,5″), 123.6 (qpy-3,3‴), 122.3 (qpy-3′,3″), 70.3, 68.7 (C_5H_4), n.o. (C_5H_4-*ipso*), 7.2 (BCH_3). Anal. Calc. for $C_{64}H_{56}B_4F_{24}Fe_2N_8P_4$ (1671.99): C, 45.98; H, 3.38; N, 6.70. Found: C, 45.66; H, 3.08; N, 6.48%. ESI-MS of **[2D]$_2$(PF$_6$)$_4$**: *m*/*z* 1527 [(M − PF$_6$)$^+$; 1%], 691 [(M − 2PF$_6$)$^{2+}$; 86%], 412 [(M − 3PF$_6$)$^{3+}$; 39%], 273 [(M − 4 PF$_6$)$^{4+}$; 3%].

GPC Analyses of [1D1](PF$_6$)$_2$ and [2D](PF$_6$)$_4$

For measurements of the individual components, 1 mg of **[1D1](PF$_6$)$_2$** and 1 mg of **[2D]$_2$(PF$_6$)$_4$** were used. Each compound was dissolved in 1 ml of acetonitrile. For the spiking of **[1D1](PF$_6$)$_2$** and **[2D]$_2$(PF$_6$)$_4$**, a solid mixture of 0.5 mg of **[1D1](PF$_6$)$_2$** and 0.5 mg of **[2D]$_2$(PF$_6$)$_4$** was dissolved in 1 ml of acetonitrile. Volume of solution used in each injection step: 10–15 µl; stationary phase: Plgel 100A, 5 µm, (300 × 7.5) mm, Agilent Technologies (Polymer Laboratories); mobile phase: acetonitrile (flow rate: 0.8 ml min^{-1}); UV detector (254 nm).

X-Ray single-crystal structure determination of [2C$_2$](PF$_6$)$_2$

A blue crystal of **[2C$_2$](PF$_6$)$_2$** was mounted on top of a glass filament on an Imaging Plate Diffraction System (Rev. 2.75, Stoe & Cie). Final lattice parameters were obtained by least squares refinement of 8000 reflections. Data were collected at 293(2) K, with a crystal-to-detector distance of 60 mm ($2.68 < \theta < 28.04°$). Data were corrected for Lorentz and polarization terms; an empirical absorption correction was applied; 26884 data measured, 10943 of them are independent reflections (R(int) = 0.0982). The structure was solved by direct methods[21] and refined against F^2 with full-matrix least-squares methods.[22] Hydrogen atoms were calculated in ideal positions (riding model). A total of 586 parameters were refined, 18.7 data per parameter, $w = 1/[\sigma^2(F_o^2) + 0.147P^2]$ where $P = (F_o^2 + 2F_o^2)/3$, shift/error <0.0001 in the last cycle of refinement, residual electron density +0.970 and −0.491 eÅ^{-3}, minimized function was $\Sigma w((F_o^2) - (F_c^2))$.[2]

CCDC reference number 174939.

See http://www.rsc.org/suppdata/dt/b1/b110993f/ for crystallographic data in CIF or other electronic format.

Electrochemistry

Materials and apparatus for electrochemistry have been described elsewhere.[23] All potential values are referred to the saturated calomel electrode (SCE).

Acknowledgements

This work was supported by the Deutsche Forschungsgemeinschaft (DFG). D. L. is grateful to the Alexander von Humboldt-Foundation for a postdoc grant. P. Z. gratefully acknowledges the financial support of the University of Siena (PAR 2001).

References

1 P. Nguyen, P. Gómez-Elipe and I. Manners, *Chem. Rev.*, 1999, **99**, 1515.
2 *Inorganic Materials*, ed. D. W. Bruce and D. O'Hare, John Wiley & Sons, Chichester, UK, 1992.
3 N. J. Long, *Angew. Chem., Int. Ed.*, 1995, **34**, 21.
4 L. Oriol and J. L. Serrano, *Adv. Mater.*, 1995, **7**, 348.
5 P. D. Beer and P. A. Gale, *Angew. Chem., Int. Ed.*, 2001, **40**, 486.
6 *Chemical Sensors*, ed. T. E. Edmonds, Blackie, Glasgow, 1988.
7 M. Fontani, F. Peters, W. Scherer, W. Wachter, M. Wagner and P. Zanello, *Eur. J. Inorg. Chem.*, 1998, 1453; M. Fontani, F. Peters,

W. Scherer, W. Wachter, M. Wagner and P. Zanello, *Eur. J. Inorg. Chem.*, 1998, 2087.
8 M. Grosche, E. Herdtweck, F. Peters and M. Wagner, *Organometallics*, 1999, **18**, 4669.
9 R. E. Dinnebier, M. Wagner, F. Peters, K. Shankland and W. I. F. David, *Z. Anorg. Allg. Chem.*, 2000, **626**, 1400.
10 T. Renk, W. Ruf and W. Siebert, *J. Organomet. Chem.*, 1976, **120**, 1.
11 W. Ruf, T. Renk and W. Siebert, *Z. Naturforsch., Teil B*, 1976, **31**, 1028.
12 F. Fabrizi de Biani, T. Gmeinwieser, E. Herdtweck, F. Jäkle, F. Laschi, M. Wagner and P. Zanello, *Organometallics*, 1997, **16**, 4776.
13 L. Ding, K. Ma, M. Bolte, F. Fabrizi de Biani, P. Zanello and M. Wagner, *J. Organomet. Chem.*, 2001, **637–639**, 390.
14 A. Neels and H. Stoeckli-Evans, *Chimia*, 1993, **47**, 198.
15 A. J. Downard, G. E. Honey, L. F. Phillips and P. J. Steel, *Inorg. Chem.*, 1991, **30**, 2260.
16 A. S. Chia and J. R. F. Trimble, *J. Phys. Chem.*, 1961, **65**, 863.
17 P. Krumholz, *J. Am. Chem. Soc.*, 1951, **73**, 3487.
18 H. Nöth and B. Wrackmeyer, Nuclear Magnetic Resonance Spectroscopy of Boron Compounds, in *NMR Basic Principles and Progress*, ed. P. Diehl, E. Fluck and R. Kosfeld, Springer, Berlin, 1978.
19 L. Ding, M. Wagner and M. Bolte, *Acta Crystallogr., Sect. C*, 2001, **57**, 162.
20 R. E. Dinnebier, L. Ding, K. Ma, M. A. Neumann, N. Tanpipat, F. J. J. Leusen, P. W. Stephens and M. Wagner, *Organometallics*, 2001, **20**, 5642.
21 G. M. Sheldrick, *Acta Crystallogr., Sect. A*, 1990, **46**, 467.
22 G. M. Sheldrick, SHELXL-97. A Program for the Refinement of Crystal Structures, Universität Göttingen, 1997.
23 R. D. Pergola, A. Cinquantini, E. Diana, L. Garlaschelli, F. Laschi, P. Luzzini, M. Manassero, A. Repossi, M. Sansoni, P. L. Stanghellini and P. Zanello, *Inorg. Chem.*, 1997, **36**, 3761.